

## CHAPTER 8

# Manipulator-mechanism design

---

8.1	INTRODUCTION
8.2	BASING THE DESIGN ON TASK REQUIREMENTS
8.3	KINEMATIC CONFIGURATION
8.4	QUANTITATIVE MEASURES OF WORKSPACE ATTRIBUTES
8.5	REDUNDANT AND CLOSED-CHAIN STRUCTURES
8.6	ACTUATION SCHEMES
8.7	STIFFNESS AND DEFLECTIONS
8.8	POSITION SENSING
8.9	FORCE SENSING

---

### 8.1 INTRODUCTION

In previous chapters, we have seen that the particular structure of a manipulator influences kinematic and dynamic analysis. For example, some kinematic configurations will be easy to solve; others will have no closed-form kinematic solution. Likewise, the complexity of the dynamic equations can vary greatly with the kinematic configuration and the mass distribution of the links. In coming chapters, we will see that manipulator control depends not only on the rigid-body dynamics, but also upon the friction and flexibility of the drive systems.

The tasks that a manipulator can perform will also vary greatly with the particular design. Although we have generally dealt with the robot manipulator as an abstract entity, its performance is ultimately limited by such pragmatic factors as load capacity, speed, size of workspace, and repeatability. For certain applications, the overall manipulator size, weight, power consumption, and cost will be significant factors.

This chapter discusses some of the issues involved in the design of the manipulator. In general, methods of design and even the evaluation of a finished design are partially subjective topics. It is difficult to narrow the spectrum of design choices with many hard and fast rules.

The elements of a robot system fall roughly into four categories:

1. The manipulator, including its internal or **proprioceptive** sensors;
2. the end-effector, or **end-of-arm tooling**;
3. external sensors and effectors, such as vision systems and part feeders; and
4. the controller.

The breadth of engineering disciplines encompassed forces us to restrict our attention only to the design of the manipulator itself.

In developing a manipulator design, we will start by examining the factors likely to have the greatest overall effect on the design and then consider more detailed questions. Ultimately, however, designing a manipulator is an iterative process. More often than not, problems that arise in the solving of a design detail will force rethinking of previous higher level design decisions.

## 8.2 BASING THE DESIGN ON TASK REQUIREMENTS

Although robots are nominally “universally programmable” machines capable of performing a wide variety of tasks, economies and practicalities dictate that different manipulators be designed for particular types of tasks. For example, large robots capable of handling payloads of hundreds of pounds do not generally have the capability to insert electronic components into circuit boards. As we shall see, not only the size, but the number of joints, the arrangement of the joints, and the types of actuation, sensing, and control will all vary greatly with the sort of task to be performed.

### Number of degrees of freedom

The number of degrees of freedom in a manipulator should match the number required by the task. Not all tasks require a full six degrees of freedom.

The most common such circumstance occurs when the end-effector has an axis of symmetry. Figure 8.1 shows a manipulator positioning a grinding tool in two different ways. In this case, the orientation of the tool with respect to the axis of the tool,  $\hat{Z}_T$ , is immaterial, because the grinding wheel is spinning at several hundred RPM. To say that we can position this 6-DOF robot in an infinity of ways for this task (rotation about  $\hat{Z}_T$  is a free variable), we say that the robot is **redundant** for this task. Arc welding, spot welding, deburring, glueing, and polishing provide other examples of tasks that often employ end-effectors with at least one axis of symmetry.

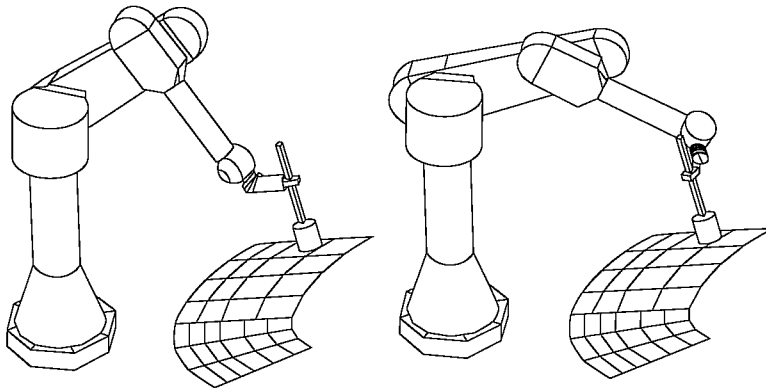


FIGURE 8.1: A 6-DOF manipulator with a symmetric tool contains a redundant degree of freedom.

In analyzing the symmetric-tool situation, it is sometimes helpful to imagine a *fictitious joint* whose axis lies along the axis of symmetry. In positioning any end-effector to a specific pose, we need a total of six degrees of freedom. Because one of these six is our fictitious joint, the actual manipulator need not have more than five degrees of freedom. If a 5-DOF robot were used in the application of Fig. 8.1, then we would be back to the usual case in which only a finite number of different solutions are available for positioning the tool. Quite a large percentage of existing industrial robots are 5-DOF, in recognition of the relative prevalence of symmetric-tool applications.

Some tasks are performed in domains that, fundamentally, have fewer than six degrees of freedom. Placement of components on circuit boards provides a common example of this. Circuit boards generally are planar and contain parts of various heights. Positioning parts on a planar surface requires three degrees of freedom ( $x$ ,  $y$ , and  $\theta$ ); in order to lift and insert the parts, a fourth motion normal to the plane is added ( $z$ ).

Robots with fewer than six degrees of freedom can also perform tasks in which some sort of active positioning device presents the parts. In welding pipes, for example, a tilt/roll platform, shown in Fig. 8.2, often presents the parts to be welded. In counting the number of degrees of freedom between the pipes and the end-effector, the tilt/roll platform accounts for two. This, together with the fact that arc welding is a symmetric-tool task, means that, in theory, a 3-DOF manipulator could be used. In practice, realities such as the need to avoid collisions with the workpiece generally dictate the use of a robot with more degrees of freedom.

Parts with an axis of symmetry also reduce the required degrees of freedom for the manipulator. For example, cylindrical parts can in many cases be picked up and inserted independent of the orientation of the gripper with respect to the axis of the cylinder. Note, however, that after the part is grasped, the orientation of the part about its symmetric axis must fail to matter for *all* subsequent operations, because its orientation is not guaranteed.

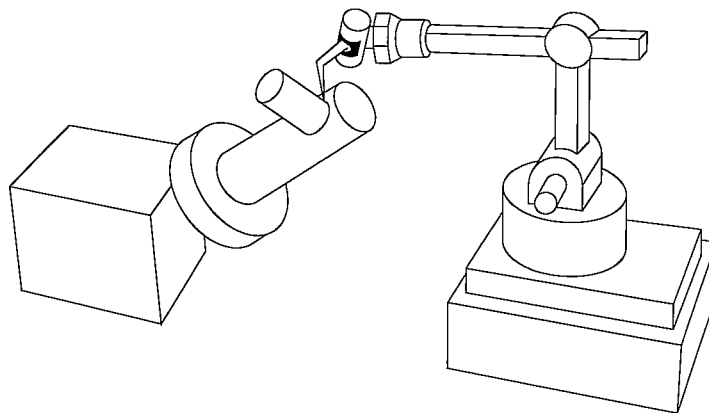


FIGURE 8.2: A tilt/roll platform provides two degrees of freedom to the overall manipulator system.

## Workspace

In performing tasks, a manipulator has to reach a number of workpieces or fixtures. In some cases, these can be positioned as needed to suit the workspace of the manipulator. In other cases, a robot can be installed in a fixed environment with rigid workspace requirements. **Workspace** is also sometimes called **work volume** or **work envelope**.

The overall scale of the task sets the required workspace of the manipulator. In some cases, the details of the shape of the workspace and the location of workspace singularities will be important considerations.

The intrusion of the manipulator itself in the workspace can sometimes be a factor. Depending on the kinematic design, operating a manipulator in a given application could require more or less space around the fixtures in order to avoid collisions. Restricted environments can affect the choice of kinematic configuration.

## Load capacity

The **load capacity** of a manipulator depends upon the sizing of its structural members, power-transmission system, and actuators. The load placed on actuators and drive system is a function of the configuration of the robot, the percentage of time supporting a load, and dynamic loading due to inertial- and velocity-related forces.

## Speed

An obvious goal in design has been for faster and faster manipulators. High speed offers advantages in many applications when a proposed robotic solution must compete on economic terms with hard automation or human workers. For some applications, however, the process itself limits the speed rather than the manipulator. This is the case with many welding and spray-painting applications.

An important distinction is that between the maximum end-effector speed and the overall **cycle time** for a particular task. For pick-and-place applications, the manipulator must accelerate and decelerate to and from the *pick* and *place* locations within some positional accuracy bounds. Often, the acceleration and deceleration phases take up most of the cycle time. Hence, acceleration capability, not just peak speed, is very important.

## Repeatability and accuracy

High repeatability and accuracy, although desirable in any manipulator design, are expensive to achieve. For example, it would be absurd to design a paint-spraying robot to be accurate to within 0.001 inches when the spray spot diameter is 8 inches  $\pm 2$  inches. To a large extent, accuracy of a particular model of industrial robot depends upon the details of its manufacture rather than on its design. High accuracy is achieved by having good knowledge of the link (and other) parameters. Making it possible are accurate measurements after manufacture or careful attention to tolerances during manufacturing.

### 8.3 KINEMATIC CONFIGURATION

Once the required number of degrees of freedom has been decided upon, a particular configuration of joints must be chosen to realize those freedoms. For serial kinematic linkages, the number of joints equals the required number of degrees of freedom. Most manipulators are designed so that the last  $n - 3$  joints orient the end-effector and have axes that intersect at the **wrist point**, and the first three joints position this wrist point. Manipulators with this design could be said to be composed of a **positioning structure** followed by an **orienting structure** or **wrist**. As we saw in Chapter 4, these manipulators always have closed-form kinematic solutions. Although other configurations exist that possess closed-form kinematic solutions, almost every industrial manipulator belongs to this **wrist-partitioned** class of mechanisms. Furthermore, the positioning structure is almost without exception designed to be kinematically simple, having link twists equal to  $0^\circ$  or  $\pm 90^\circ$  and having many of the link lengths and offsets equal to zero.

It has become customary to classify manipulators of the wrist-partitioned, kinematically simple class according to the design of their first three joints (the positioning structure). The following paragraphs briefly describe the most common of these classifications.

#### Cartesian

A **Cartesian manipulator** has perhaps the most straightforward configuration. As shown in Fig. 8.3, joints 1 through 3 are prismatic, mutually orthogonal, and correspond to the  $\hat{X}$ ,  $\hat{Y}$ , and  $\hat{Z}$  Cartesian directions. The inverse kinematic solution for this configuration is trivial.

This configuration produces robots with very stiff structures. As a consequence, very large robots can be built. These large robots, often called **gantry robots**, resemble overhead gantry cranes. Gantry robots sometimes manipulate entire automobiles or inspect entire aircraft.

The other advantages of Cartesian manipulators stem from the fact that the first three joints are *decoupled*. This makes them simpler to design and prevents kinematic singularities due to the first three joints.

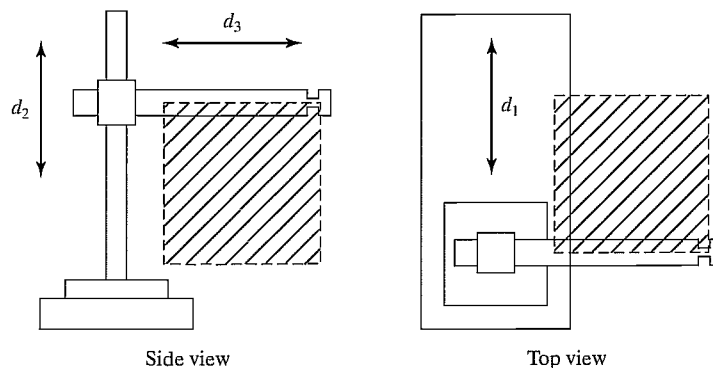


FIGURE 8.3: A Cartesian manipulator.

Their primary disadvantage is that all of the feeders and fixtures associated with an application must lie “inside” the robot. Consequently, application workcells for Cartesian robots become very machine dependent. The size of the robot’s support structure limits the size and placement of fixtures and sensors. These limitations make retrofitting Cartesian robots into existing workcells extremely difficult.

### Articulated

Figure 8.4 shows an **articulated manipulator**, sometimes also called a **jointed, elbow**, or **anthropomorphic** manipulator. A manipulator of this kind typically consists of two “shoulder” joints (one for rotation about a vertical axis and one for elevation out of the horizontal plane), an “elbow” joint (whose axis is usually parallel to the shoulder elevation joint), and two or three wrist joints at the end of the manipulator. Both the PUMA 560 and the Motoman L-3, which we studied in earlier chapters, fall into this class.

Articulated robots minimize the intrusion of the manipulator structure into the workspace, making them capable of reaching into confined spaces. They require much less overall structure than Cartesian robots, making them less expensive for applications needing smaller workspaces.

### SCARA

The **SCARA**<sup>1</sup> configuration, shown in Fig. 8.5, has three parallel revolute joints (allowing it to move and orient in a plane), with a fourth prismatic joint for moving the end-effector normal to the plane. The chief advantage is that the first three joints don’t have to support any of the weight of the manipulator or the load. In addition, link 0 can easily house the actuators for the first two joints. The actuators can be made very large, so the robot can move very fast. For example, the Adept

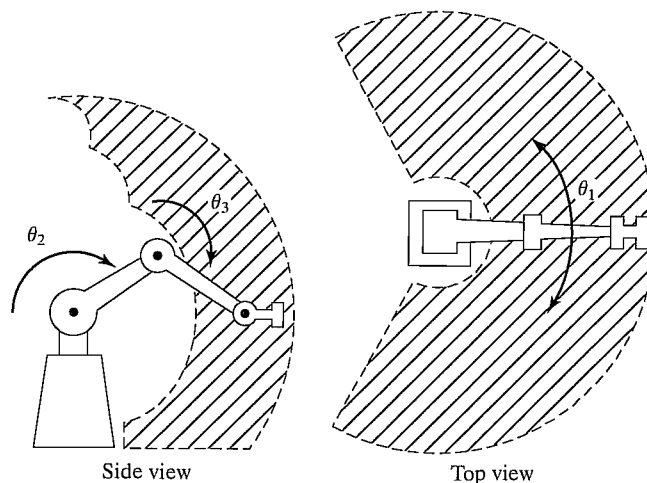


FIGURE 8.4: An articulated manipulator.

<sup>1</sup>SCARA stands for “selectively compliant assembly robot arm.”

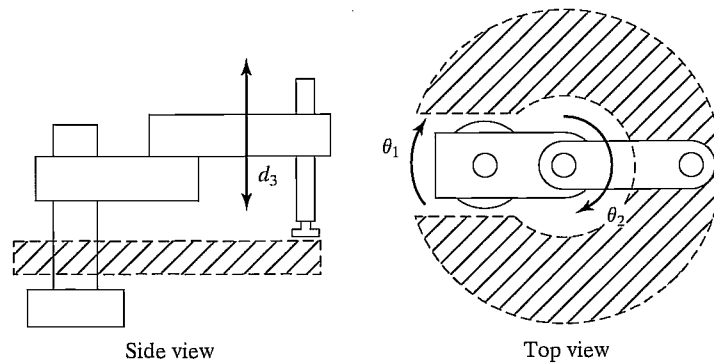


FIGURE 8.5: A SCARA manipulator.

One SCARA manipulator can move at up to 30 feet per second, about 10 times faster than most articulated industrial robots [1]. This configuration is best suited to planar tasks.

### Spherical

The spherical configuration in Fig. 8.6 has many similarities to the articulated manipulator, but with the elbow joint replaced by a prismatic joint. This design is better suited to some applications than is the elbow design. The link that moves prismatically might telescope—or even “stick out the back” when retracted.

### Cylindrical

**Cylindrical** manipulators (Fig. 8.7) consist of a prismatic joint for translating the arm vertically, a revolute joint with a vertical axis, another prismatic joint orthogonal to the revolute joint axis, and, finally, a wrist of some sort.

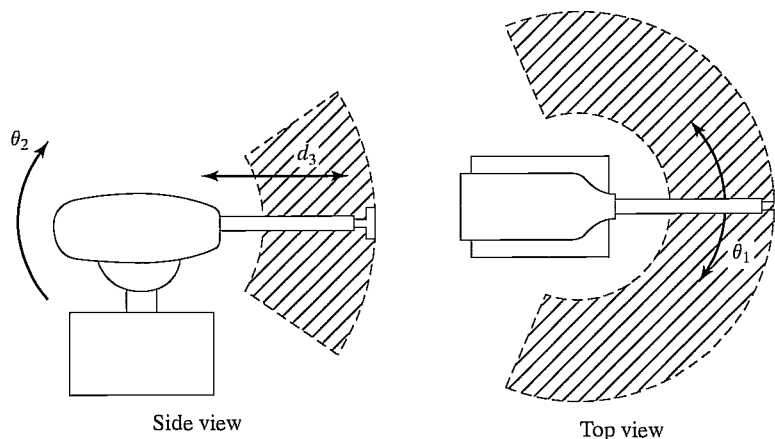


FIGURE 8.6: A spherical manipulator.

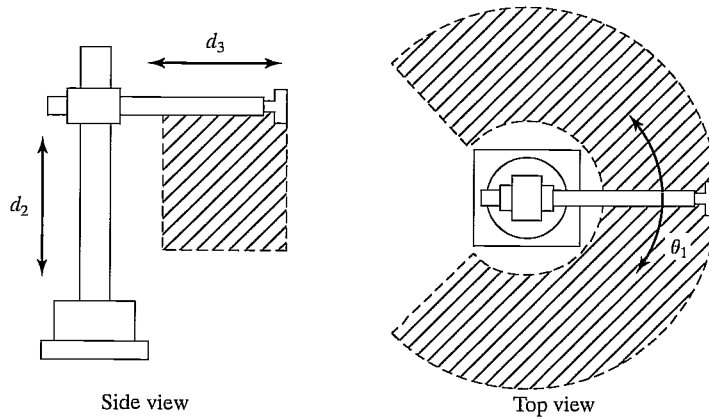


FIGURE 8.7: A cylindrical manipulator.

### Wrists

The most common wrist configurations consist of either two or three revolute joints with orthogonal, intersecting axes. The first of the wrist joints usually forms joint 4 of the manipulator.

A configuration of three orthogonal axes will guarantee that any orientation can be achieved (assuming no joint-angle limits) [2]. As was stated in Chapter 4, any manipulator with three consecutive intersecting axes will possess a closed-form kinematic solution. Therefore, a three-orthogonal-axis wrist can be located at the end of the manipulator in any desired orientation with no penalty. Figure 8.8 is a schematic of one possible design of such a wrist, which uses several sets of bevel gears to drive the mechanism from remotely located actuators.

In practice, it is difficult to build a three-orthogonal-axis wrist not subject to rather severe joint-angle limitations. An interesting design used in several robots

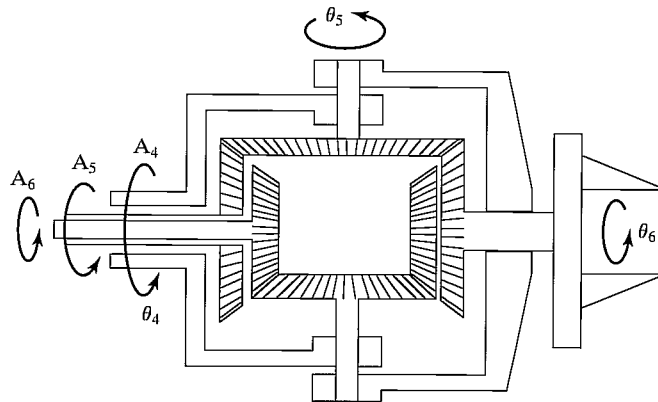


FIGURE 8.8: An orthogonal-axis wrist driven by remotely located actuators via three concentric shafts.

manufactured by Cincinatti Milacron (Fig. 1.4) employs a wrist that has three intersecting but nonorthogonal axes. In this design (called the “three roll wrist”), all three joints of the wrist can rotate continuously without limits. The nonorthogonality of the axes creates, however, a set of orientations that are impossible to reach with this wrist. This set of unattainable orientations is described by a cone within which the third axis of the wrist cannot lie. (See Exercise 8.11.) However, the wrist can be mounted to link 3 of the manipulator in such a way that the link structure occupies this cone and so would be block access anyway. Figure 8.9 shows two drawings of such a wrist [24].

Some industrial robots have wrists that do *not* have intersecting axes. This implies that a closed-form kinematic solution might not exist. If, however, the wrist is mounted on an articulated manipulator in such a way that the joint-4 axis is parallel to the joint-2 and -3 axes, as in Fig. 8.10, there *will* be a closed-form kinematic solution. Likewise, a nonintersecting-axis wrist mounted on a Cartesian robot yields a closed-form-solvable manipulator.

Typically, 5-DOF welding robots use two-axis wrists oriented as shown in Fig. 8.11. Note that, if the robot has a symmetric tool, this “fictitious joint” must follow the rules of wrist design. That is, in order to reach all orientations, the tool must be mounted with its axis of symmetry orthogonal to the joint-5 axis. In the worst case, when the axis of symmetry is parallel to the joint-5 axis, the fictitious sixth axis is in a permanently singular configuration.

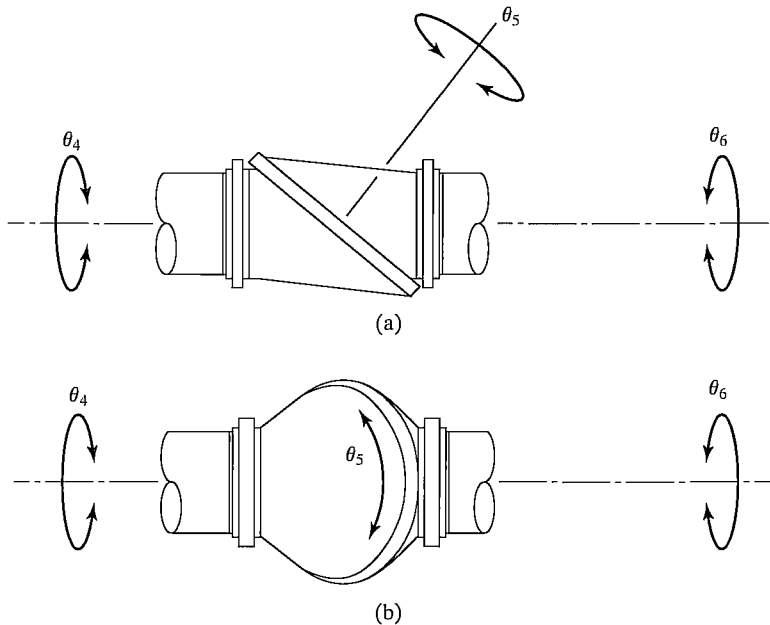


FIGURE 8.9: Two views of a nonorthogonal-axis wrist [24]. From *International Encyclopedia of Robotics*, by R. Dorf and S. Nof (editors). From “Wrists” by M. Rosheim, John C. Wiley and Sons, Inc., New York, NY ©1988. Reprinted by permission.

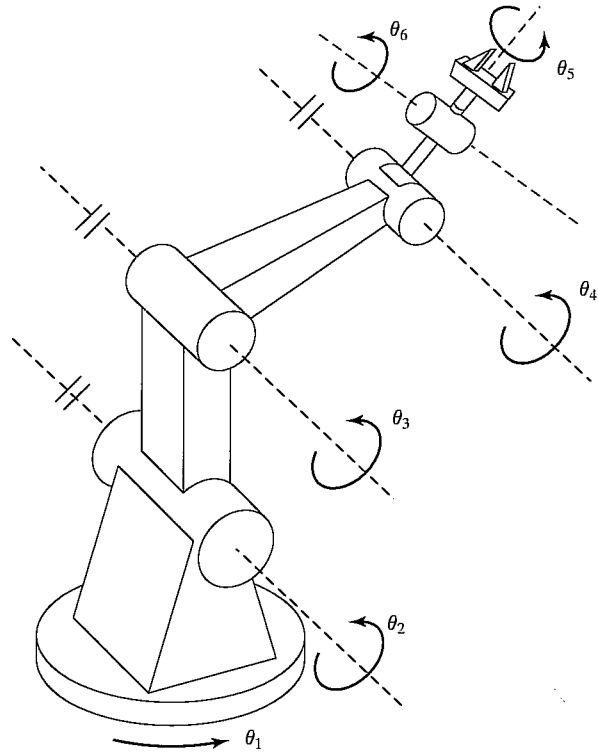


FIGURE 8.10: A manipulator with a wrist whose axes do not intersect. However, this robot does possess a closed-form kinematic solution.

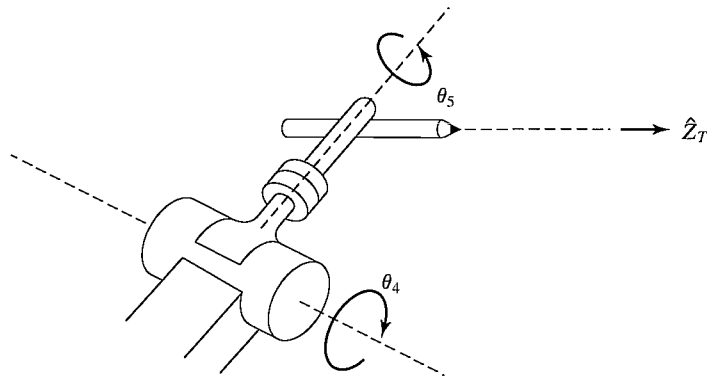


FIGURE 8.11: Typical wrist design of a 5-DOF welding robot.

## 8.4 QUANTITATIVE MEASURES OF WORKSPACE ATTRIBUTES

Manipulator designers have proposed several interesting quantitative measures of various workspace attributes.

**Efficiency of design in terms of generating workspace**

Some designers noticed that it seemed to take more material to build a Cartesian manipulator than to build an articulated manipulator of similar workspace volume. To get a quantitative handle on this, we first define the **length sum** of a manipulator as

$$L = \sum_{i=1}^N (a_{i-1} + d_i), \quad (8.1)$$

where  $a_{i-1}$  and  $d_i$  are the link length and joint offset as defined in Chapter 3. Thus, the length sum of a manipulator gives a rough measure of the “length” of the complete linkage. Note that, for prismatic joints,  $d_i$  must here be interpreted as a constant equal to the length of travel between the joint-travel limits.

In [3], the **structural length index**,  $Q_L$ , is defined as the ratio of the manipulator’s length sum to the cube root of the workspace volume—that is,

$$Q_L = L/\sqrt[3]{w}, \quad (8.2)$$

where  $L$  is given in (8.1) and  $W$  is the volume of the manipulator’s workspace. Hence,  $Q_L$  attempts to index the relative amount of structure (linkage length) required by different configurations to generate a given work volume. Thus, a good design would be one in which a manipulator with a small length sum nonetheless possessed a large workspace volume. Good designs have a low  $Q_L$ .

Considering just the positioning structure of a Cartesian manipulator (and therefore the workspace of the wrist point), the value of  $Q_L$  is minimized when all three joints have the same length of travel. This minimal value is  $Q_L = 3.0$ . On the other hand, an ideal articulated manipulator, such as the one in Fig. 8.4, has  $Q_L = \frac{1}{\sqrt[3]{4\pi/3}} \cong 0.62$ . This helps quantify our earlier statement that articulated manipulators are superior to other configurations in that they have minimal intrusion into their own workspace. Of course, in any real manipulator structure, the figure just given would be made somewhat larger by the effect of joint limits in reducing the workspace volume.

**EXAMPLE 8.1**

A SCARA manipulator like that of Fig. 8.5 has links 1 and 2 of equal length  $l/2$ , and the range of motion of the prismatic joint 3 is given by  $d_3$ . Assume for simplicity that the joint limits are absent, and find  $Q_L$ . What value of  $d_3$  minimizes  $Q_L$  and what is this minimal value?

The length sum of this manipulator is  $L = l/2 + l/2 + d_3 = l + d_3$ , and the workspace volume is that of a right cylinder of radius  $l$  and height  $d_3$ ; therefore,

$$Q_L = \frac{l + d_3}{\sqrt[3]{\pi l^2 d_3}}. \quad (8.3)$$

Minimizing  $Q_L$  as a function of the ratio  $d_3/l$  gives  $d_3 = l/2$  as optimal [3]. The corresponding minimal value of  $Q_L$  is 1.29.

### Designing well-conditioned workspaces

At singular points, a manipulator effectively loses one or more degrees of freedom, so certain tasks may not be able to be performed at that point. In fact, in the neighborhood of singular points (including workspace-boundary singularities), actions of the manipulator could fail to be **well-conditioned**. In some sense, the farther the manipulator is away from singularities, the better able it is to move uniformly and apply forces uniformly in all directions. Several measures have been suggested for quantifying this effect. The use of such measures at design time might yield a manipulator design with a maximally large well-conditioned subspace of the workspace.

Singular configurations are given by

$$\det(J(\Theta)) = 0, \quad (8.4)$$

so it is natural to use the determinant of the Jacobian in a measure of manipulator dexterity. In [4], the **manipulability measure**,  $w$ , is defined as

$$w = \sqrt{\det(J(\Theta)J^T(\Theta))}, \quad (8.5)$$

which, for a nonredundant manipulator, reduces to

$$w = |\det(J(\Theta))|. \quad (8.6)$$

A good manipulator design has large areas of its workspace characterized by high values of  $w$ .

Whereas velocity analysis motivated (8.6), other researchers have proposed manipulability measures based on acceleration analysis or force-application capability. Asada [5] suggested an examination of the eigenvalues of the Cartesian mass matrix

$$M_x(\Theta) = J^{-T}(\Theta)M(\Theta)J^{-1}(\Theta) \quad (8.7)$$

as a measure of how well the manipulator can accelerate in various Cartesian directions. He suggests a graphic representation of this measure as an **inertia ellipsoid**, given by

$$X^T M_x(\Theta)X = 1, \quad (8.8)$$

the equation of an  $n$ -dimensional ellipse, where  $n$  is the dimension of  $X$ . The axes of the ellipsoid given in (8.8) lie in the directions of the eigenvectors of  $M_x(\Theta)$ , and the reciprocals of the square roots of the corresponding eigenvalues provide the lengths of the axes of the ellipsoid. Well-conditioned points in the manipulator workspace are characterized by inertia ellipsoids that are spherical (or nearly so).

Figure 8.12 shows graphically the properties of a planar two-link manipulator. In the center of the workspace, the manipulator is well conditioned, as is indicated by nearly circular ellipsoids. At workspace boundaries, the ellipses flatten, indicating the manipulator's difficulty in accelerating in certain directions.

Other measures of workspace conditioning have been proposed in [6–8, 25].

## 8.5 REDUNDANT AND CLOSED-CHAIN STRUCTURES

In general, the scope of this book is limited to manipulators that are serial-chain linkages of six or fewer joints. In this section, however, we briefly discuss manipulators outside of this class.

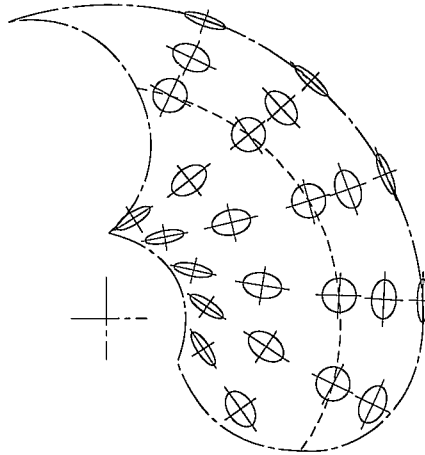


FIGURE 8.12: Workspace of a 2-DOF planar arm, showing inertia ellipsoids, from [5] (© 1984 IEEE). The dashed line indicates a locus of isotropic points in the workspace. Reprinted by permission.

### Micromanipulators and other redundancies

General spatial positioning capability requires only six degrees of freedom, but there are advantages to having even more controllable joints.

One use for these extra freedoms is already finding some practical application [9,10] and is of growing interest in the research community: a **micromanipulator**. A micromanipulator is generally formed by several fast, precise degrees of freedom located near the distal end of a “conventional” manipulator. The conventional manipulator takes care of large motions, while the micromanipulator, whose joints generally have a small range of motion, accomplishes fine motion and force control.

Additional joints can also help a mechanism avoid singular configurations, as is suggested in [11, 12]. For example, any three-degree-of-freedom wrist will suffer from singular configurations (when all three axes lie in a plane), but a four-degree-of-freedom wrist can effectively avoid such configurations [13–15].

Figure 8.13 shows two configurations suggested [11, 12] for seven-degree-of-freedom manipulators.

A major potential use of redundant robots is in avoiding collisions while operating in cluttered work environments. As we have seen, a six-degree-of-freedom manipulator can reach a given position and orientation in only a finite number of ways. The addition of a seventh joint allows an infinity of ways, permitting the desire to avoid obstacles to influence the choice.

### Closed-loop structures

Although we have considered only serial-chain manipulators in our analysis, some manipulators contain **closed-loop structures**. For example, the Motoman L-3 robot described in Chapters 3 and 4 possesses closed-loop structures in the drive mechanism of joints 2 and 3. Closed-loop structures offer a benefit: increased stiffness of

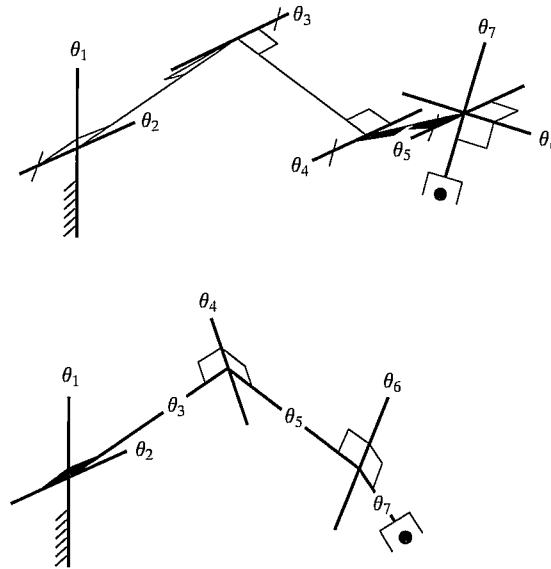


FIGURE 8.13: Two suggested seven-degree-of-freedom manipulator designs [3].

the mechanism [16]. On the other hand, closed-loop structures generally reduce the allowable range of motion of the joints and thus decrease the workspace size.

Figure 8.14 depicts a **Stewart mechanism**, a closed-loop alternative to the serial 6-DOF manipulator. The position and orientation of the “end-effector” is controlled by the lengths of the six linear actuators which connect it to the base. At the base end, each actuator is connected by a two-degree-of-freedom universal joint. At the end-effector, each actuator is attached with a three-degree-of-freedom ball-and-socket joint. It exhibits characteristics common to most closed-loop mechanisms: it can be made very stiff, but the links have a much more limited range of motion than do serial linkages. The Stewart mechanism, in particular, demonstrates an interesting reversal in the nature of the forward and inverse kinematic solutions: the inverse solution is quite simple, whereas the forward solution is typically quite complex, sometimes lacking a closed-form formulation. (See Exercises 8.7 and 8.12.)

In general, the number of degrees of freedom of a closed-loop mechanism is not obvious. The total number of degrees of freedom can be computed by means of **Grübler’s** formula [17],

$$F = 6(l - n - 1) + \sum_{i=1}^n f_i, \quad (8.9)$$

where  $F$  is the total number of degrees of freedom in the mechanism,  $l$  is the number of links (including the base),  $n$  is the total number of joints, and  $f_i$  is the number of degrees of freedom associated with the  $i$ th joint. A planar version of Grübler’s formula (when all objects are considered to have three degrees of freedom if unconstrained) is obtained by replacing the 6 in (8.9) with a 3.

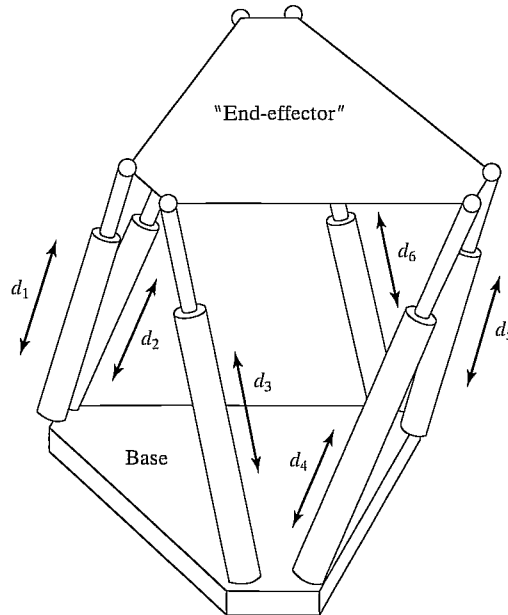


FIGURE 8.14: The Stewart mechanism is a six-degree-of-freedom fully parallel manipulator.

---

### EXAMPLE 8.2

Use Grübler's formula to verify that the Stewart mechanism (Fig. 8.14) indeed has six degrees of freedom.

The number of joints is 18 (6 universal, 6 ball and socket, and 6 prismatic in the actuators). The number of links is 14 (2 parts for each actuator, the end-effector, and the base). The sum of all the joint freedoms is 36. Using Grübler's formula, we can verify that the total number of degrees of freedom is six:

$$F = 6(14 - 18 - 1) + 36 = 6. \quad (8.10)$$


---

## 8.6 ACTUATION SCHEMES

Once the general kinematic structure of a manipulator has been chosen, the next most important matter of concern is the actuation of the joints. Typically, the actuator, reduction, and transmission are closely coupled and must be designed together.

### Actuator location

The most straightforward choice of actuator location is at or near the joint it drives. If the actuator can produce enough torque or force, its output can attach directly to the joint. This arrangement, known as a **direct-drive** configuration [18], offers

the advantages of simplicity in design and superior controllability—that is, with no transmission or reduction elements between the actuator and the joint, the joint motions can be controlled with the same fidelity as the actuator itself.

Unfortunately, many actuators are best suited to relatively high speeds and low torques and therefore require a **speed-reduction system**. Furthermore, actuators tend to be rather heavy. If they can be located remotely from the joint and toward the base of the manipulator, the overall inertia of the manipulator can be reduced considerably. This, in turn, reduces the size needed for the actuators. To realize these benefits, a **transmission system** is needed to transfer the motion from the actuator to the joint.

In a joint-drive system with a remotely mounted actuator, the reduction system could be placed either at the actuator or at the joint. Some arrangements combine the functions of transmission and reduction. Aside from added complexity, the major disadvantage of reduction and transmission systems is that they introduce additional friction and flexibility into the mechanism. When the reduction is at the joint, the transmission will be working at higher speeds and lower torques. Lower torque means that flexibility will be less of a problem. However, if the weight of the reducer is significant, some of the advantage of remotely mounted actuators is lost.

In Chapter 3, details were given for the actuation scheme of the Yasukawa Motoman L-3, which is typical of a design in which actuators are mounted remotely and resulting joint motions are coupled. Equations (3.16) show explicitly how actuator motions cause joint motions. Note, for example, that motion of actuator 2 causes motion of joints 2, 3, and 4.

The optimal distribution of reduction stages throughout the transmission will depend ultimately on the flexibility of the transmission, the weight of the reduction system, the friction associated with the reduction system, and the ease of incorporating these components into the overall manipulator design.

### Reduction and transmission systems

**Gears** are the most common element used for reduction. They can provide for large reductions in relatively compact configurations. Gear pairs come in various configurations for parallel shafts (spur gears), orthogonal intersecting shafts (bevel gears), skew shafts (worm gears or cross helical gears), and other configurations. Different types of gears have different load ratings, wear characteristics, and frictional properties.

The major disadvantages of using gearing are added **backlash** and friction. Backlash, which arises from the imperfect meshing of gears, can be defined as the maximum angular motion of the output gear when the input gear remains fixed. If the gear teeth are meshed tightly to eliminate backlash, there can be excessive amounts of friction. Very precise gears and very precise mounting minimize these problems, but also increase cost.

The **gear ratio**,  $\eta$ , describes the speed-reducing and torque-increasing effects of a gear pair. For speed-reduction systems, we will define  $\eta > 1$ ; then the relationships between input and output speeds and torques are given by

$$\begin{aligned}\dot{\theta}_o &= (1/\eta)\dot{\theta}_i \\ \tau_o &= \eta\tau_i,\end{aligned}\tag{8.11}$$

where  $\dot{\theta}_o$  and  $\dot{\theta}_i$  are output and input speeds, respectively, and  $\tau_o$  and  $\tau_i$  are output and input torques, respectively.

The second broad class of reduction elements includes flexible bands, cables, and belts. Because all of these elements must be flexible enough to bend around pulleys, they also tend to be flexible in the longitudinal direction. The flexibility of these elements is proportional to their length. Because these systems are flexible, there must be some mechanism for preloading the loop to ensure that the belt or cable stays engaged on the pulley. Large preloads can add undue strain to the flexible element and introduce excessive friction.

Cables or flexible bands can be used either in a closed loop or as single-ended elements that are always kept in tension by some sort of preload. In a joint that is spring loaded in one direction, a single-ended cable could be used to pull against it. Alternately, two active single-ended systems can oppose each other. This arrangement eliminates the problem of excessive preloads but adds more actuators.

Roller chains are similar to flexible bands but can bend around relatively small pulleys while retaining a high stiffness. As a result of wear and high loads on the pins connecting the links, toothed-belt systems are more compact than roller chains for certain applications.

Band, cable, belt, and chain drives have the ability to combine transmission with reduction. As is shown in Fig. 8.15, when the input pulley has radius  $r_1$  and the output pulley has radius  $r_2$ , the “gear” ratio of the transmission system is

$$\eta = \frac{r_2}{r_1}. \quad (8.12)$$

Lead screws or ball-bearing screws provide another popular method of getting a large reduction in a compact package (Fig. 8.16). Lead screws are very stiff and can support very large loads, and have the property that they transform rotary motion into linear motion. Ball-bearing screws are similar to lead screws, but instead of having the nut threads riding directly on the screw threads, a recirculating circuit of ball bearings rolls between the sets of threads. Ball-bearing screws have very low friction and are usually backdrivable.

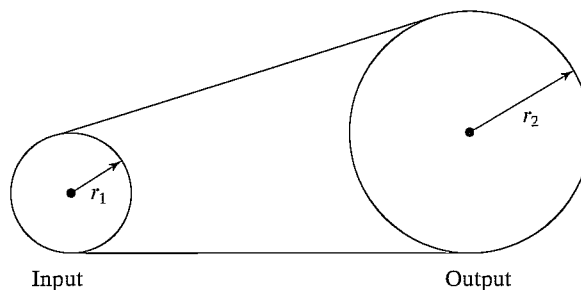


FIGURE 8.15: Band, cable, belt, and chain drives have the ability to combine transmission with reduction.

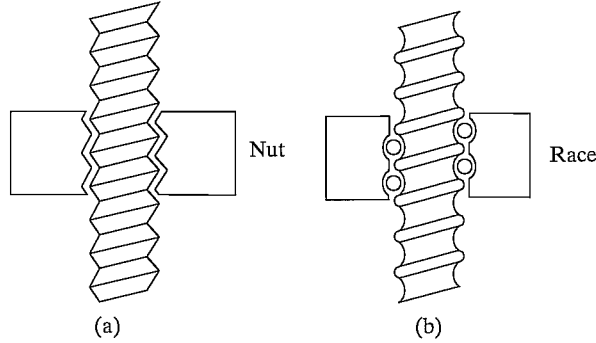


FIGURE 8.16: Lead screws (a) and ball-bearing screws (b) combine a large reduction and transformation from rotary to linear motion.

## 8.7 STIFFNESS AND DEFLECTIONS

An important goal for the design of most manipulators is overall stiffness of the structure and the drive system. Stiff systems provide two main benefits. First, because typical manipulators do not have sensors to measure the tool frame location directly, it is calculated by using the forward kinematics based on sensed joint positions. For an accurate calculation, the links cannot sag under gravity or other loads. In other words, we wish our Denavit–Hartenberg description of the linkages to remain fixed under various loading conditions. Second, flexibilities in the structure or drive train will lead to **resonances**, which have an undesirable effect on manipulator performance. In this section, we consider issues of stiffness and the resulting deflections under loads. We postpone further discussion of resonances until Chapter 9.

### Flexible elements in parallel and in series

As can be easily shown (see Exercise 8.21), the combination of two flexible members of stiffness  $k_1$  and  $k_2$  “connected in parallel” produces the net stiffness

$$k_{\text{parallel}} = k_1 + k_2; \quad (8.13)$$

“connected in series,” the combination produces the net stiffness

$$\frac{1}{k_{\text{series}}} = \frac{1}{k_1} + \frac{1}{k_2}. \quad (8.14)$$

In considering transmission systems, we often have the case of one stage of reduction or transmission in series with a following stage of reduction or transmission; hence, (8.14) becomes useful.

### Shafts

A common method for transmitting rotary motion is through shafts. The torsional stiffness of a round shaft can be calculated [19] as

$$k = \frac{G\pi d^4}{32l}, \quad (8.15)$$

where  $d$  is the shaft diameter,  $l$  is the shaft length, and  $G$  is the shear modulus of elasticity (about  $7.5 \times 10^{10}$  Nt/m<sup>2</sup> for steel, and about a third as much for aluminum).

### Gears

Gears, although typically quite stiff, introduce compliance into the drive system. An approximate formula to estimate the stiffness of the output gear (assuming the input gear is fixed) is given in [20] as

$$k = C_g b r^2, \quad (8.16)$$

where  $b$  is the face width of the gears,  $r$  is the radius of the output gear, and  $C_g = 1.34 \times 10^{10}$  Nt/m<sup>2</sup> for steel.

Gearing also has the effect of changing the effective stiffness of the drive system by a factor of  $\eta^2$ . If the stiffness of the transmission system prior to the reduction (i.e., on the input side) is  $k_i$ , so that

$$\tau_i = k_i \delta\theta_i, \quad (8.17)$$

and the stiffness of the output side of the reduction is  $k_o$ , so that

$$\tau_o = k_o \delta\theta_o, \quad (8.18)$$

then we can compute the relationship between  $k_i$  and  $k_o$  (under the assumption of a perfectly rigid gear pair) as

$$k_o = \frac{\tau_o}{\delta\theta_o} = \frac{\eta k_i \delta\theta_i}{(1/\eta) \delta\theta_i} = \eta^2 k_i. \quad (8.19)$$

Hence, a gear reduction has the effect of increasing the stiffness by the square of the gear ratio.

### EXAMPLE 8.3

A shaft with torsional stiffness equal to 500.0 Nt-m/radian is connected to the input side of a gear set with  $\eta = 10$ , whose output gear (when the input gear is fixed) exhibits a stiffness of 5000.0 Nt m/radian. What is the output stiffness of the combined drive system?

Using (8.14) and (8.19), we have

$$\frac{1}{k_{\text{series}}} = \frac{1}{5000.0} + \frac{1}{10^2(500.0)}, \quad (8.20)$$

or

$$k_{\text{series}} = \frac{50000}{11} \cong 4545.4 \text{ Nt m/radian}. \quad (8.21)$$

When a relatively large speed reduction is the last element of a multielement transmission system, the stiffnesses of the preceding elements can generally be ignored.

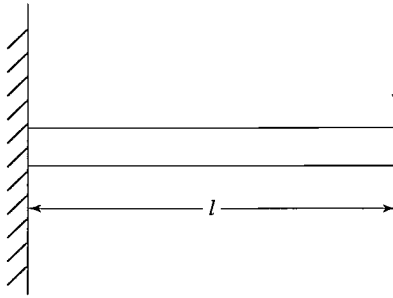


FIGURE 8.17: Simple cantilever beam used to model the stiffness of a link to an end load.

### Belts

In such a belt drive as that of Fig. 8.15, stiffness is given by

$$k = \frac{AE}{l}, \quad (8.22)$$

where  $A$  is the cross-sectional area of the belt,  $E$  is the modulus of elasticity of the belt, and  $l$  is the length of the free belt between pulleys plus one-third of the length of the belt in contact with the pulleys [19].

### Links

As a rough approximation of the stiffness of a link, we might model a single link as a cantilever beam and calculate the stiffness at the end point, as in Fig. 8.17. For a round hollow beam, this stiffness is given by [19]

$$k = \frac{3\pi E(d_o^4 - d_i^4)}{64l^3}, \quad (8.23)$$

where  $d_i$  and  $d_o$  are the inner and outer diameters of the tubular beam,  $l$  is the length, and  $E$  is the modulus of elasticity (about  $2 \times 10^{11}$  Nt/m<sup>2</sup> for steel, and about a third as much for aluminum). For a square-cross-section hollow beam, this stiffness is given by

$$k = \frac{E(w_o^4 - w_i^4)}{4l^3}, \quad (8.24)$$

where  $w_i$  and  $w_o$  are the outer and inner widths of the beam (i.e., the wall thickness is  $w_o - w_i$ ).

---

### EXAMPLE 8.4

A square-cross-section link of dimensions  $5 \times 5 \times 50$  cm with a wall thickness of 1 cm is driven by a set of rigid gears with  $\eta = 10$ , and the input of the gears is driven by a shaft having diameter 0.5 cm and length 30 cm. What deflection is caused by a force of 100 Nt at the end of the link?

Using (8.24), we calculate the stiffness of the link as

$$k_{\text{link}} = \frac{(2 \times 10^{11})(0.05^4 - 0.04^4)}{4(0.5)} \cong 3.69 \times 10^5. \quad (8.25)$$

Hence, for a load of 100 Nt, there is a deflection in the link itself of

$$\delta x = \frac{100}{k_{\text{link}}} \cong 2.7 \times 10^{-4} \text{ m}, \quad (8.26)$$

or 0.027 cm.

Additionally, 100 Nt at the end of a 50-cm link is placing a torque of 50 Nt-m on the output gear. The gears are rigid, but the flexibility of the input shaft is

$$k_{\text{shaft}} = \frac{(7.5 \times 10^{10})(3.14)(5 \times 10^{-3})^4}{(32)(0.3)} \cong 15.3 \text{ Nt m/radian}, \quad (8.27)$$

which, viewed from the output gear, is

$$k'_{\text{shaft}} = (15.3)(10^2) = 1530.0 \text{ Nt-m/radian}. \quad (8.28)$$

Loading with 50 Nt-m causes an angular deflection of

$$\delta\theta = \frac{50.0}{1530.0} \cong 0.0326 \text{ radian}, \quad (8.29)$$

so the total linear deflection at the tip of the link is

$$\delta x \cong 0.027 + (0.0326)(50) = 0.027 + 1.630 = 1.657 \text{ cm}. \quad (8.30)$$

In our solution, we have assumed that the shaft and link are made of steel. The stiffness of both members is linear in  $E$ , the modulus of elasticity, so, for aluminum elements, we can multiply our result by about 3.

---

In this section, we have examined some simple formulas for estimating the stiffness of gears, shafts, belts, and links. They are meant to give some guidance in sizing structural members and transmission elements. However, in practical applications, many sources of flexibility are very difficult to model. Often, the drive train introduces significantly more flexibility than the link of a manipulator. Furthermore, many sources of flexibility in the drive system have not been considered here (bearing flexibility, flexibility of the actuator mounting, etc.). Generally, any attempt to predict stiffness analytically results in an overly high prediction, because many sources are not considered.

**Finite-element techniques** can be used to predict the stiffness (and other properties) of more realistic structural elements more accurately. This is an entire field in itself [21] and is beyond the scope of this book.

## Actuators

Among various actuators, **hydraulic cylinders** or **vane actuators** were originally the most popular for use in manipulators. In a relatively compact package, they

can produce enough force to drive joints without a reduction system. The speed of operation depends upon the pump and accumulator system, usually located remotely from the manipulator. The position control of hydraulic systems is well understood and relatively straightforward. All of the early industrial robots and many modern large industrial robots use hydraulic actuators.

Unfortunately, hydraulics require a great deal of equipment, such as pumps, accumulators, hoses, and servo valves. Hydraulic systems also tend to be inherently messy, making them unsuitable for some applications. With the advent of more advanced robot-control strategies, in which actuator forces must be applied accurately, hydraulics proved disadvantageous, because of the friction contributed by their seals.

**Pneumatic cylinders** possess all the favorable attributes of hydraulics, and they are cleaner than hydraulics—air seeps out instead of hydraulic fluid. However, pneumatic actuators have proven difficult to control accurately, because of the compressibility of air and the high friction of the seals.

Electric motors are the most popular actuator for manipulators. Although they don't have the power-to-weight ratio of hydraulics or pneumatics, their controllability and ease of interface makes them attractive for small-to-medium-sized manipulators.

Direct current (DC) brush motors (Fig. 8.18) are the most straightforward to interface and control. The current is conducted to the windings of the rotor via brushes, which make contact with the revolving commutator. Brush wear and friction can be problems. New magnetic materials have made high peak torques possible. The limiting factor on the torque output of these motors is the overheating

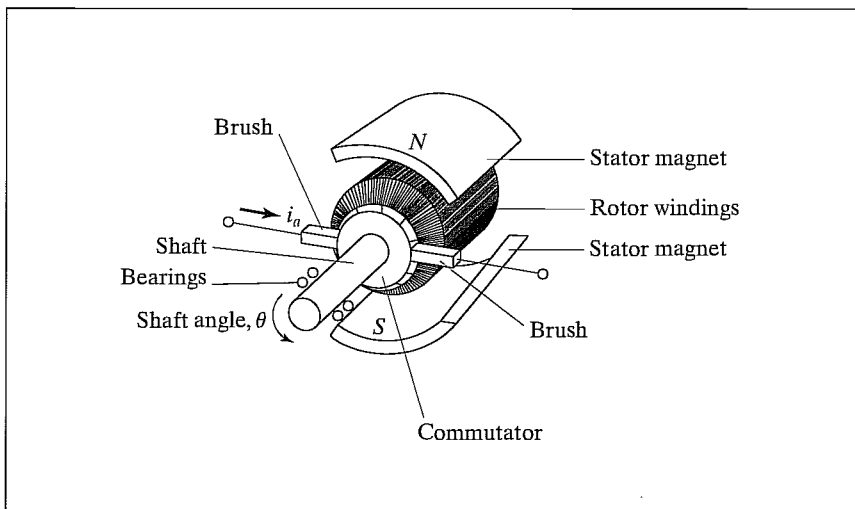


FIGURE 8.18: DC brush motors are among the actuators occurring most frequently in manipulator design. Franklin, Powell, Emami-Naeini, *Feedback Control of Dynamic Systems*, © 1988, Addison-Wesley, Reading, MA. Reprinted with permission.

of the windings. For short duty cycles, high torques can be achieved, but only much lower torques can be sustained over long periods of time.

**Brushless motors** solve brush wear and friction problems. Here, the windings remain stationary and the magnetic field piece rotates. A sensor on the rotor detects the shaft angle and is then used by external electronics to perform the commutation. Another advantage of brushless motors is that the winding is on the outside, attached to the motor case, affording it much better cooling. Sustained torque ratings tend to be somewhat higher than for similar-sized brush motors.

Alternating current (AC) motors and stepper motors have been used infrequently in industrial robotics. Difficulty of control of the former and low torque ability of the latter have limited their use.

## 8.8 POSITION SENSING

Virtually all manipulators are servo-controlled mechanisms—that is, the force or torque command to an actuator is based on the error between the sensed position of the joint and the desired position. This requires that each joint have some sort of position-sensing device.

The most common approach is to locate a position sensor directly on the shaft of the actuator. If the drive train is stiff and has no backlash, the true joint angles can be calculated from the actuator shaft positions. Such **co-located** sensor and actuator pairs are easiest to control.

The most popular position-feedback device is the **rotary optical encoder**. As the encoder shaft turns, a disk containing a pattern of fine lines interrupts a light beam. A photodetector turns these light pulses into a binary waveform. Typically, there are two such channels, with wave pulse trains 90 degrees out of phase. The shaft angle is determined by counting the number of pulses, and the direction of rotation is determined by the relative phase of the two square waves. Additionally, encoders generally emit an **index pulse** at one location, which can be used to set a home position in order to compute an absolute angular position.

**Resolvers** are devices that output two analog signals—one the sine of the shaft angle, the other the cosine. The shaft angle is computed from the relative magnitude of the two signals. The resolution is a function of the quality of the resolver and the amount of noise picked up in the electronics and cabling. Resolvers are often more reliable than optical encoders, but their resolution is lower. Typically, resolvers cannot be placed directly at the joint without additional gearing to improve the resolution.

**Potentiometers** provide the most straightforward form of position sensing. Connected in a bridge configuration, they produce a voltage proportional to the shaft position. Difficulties with resolution, linearity, and noise susceptibility limit their use.

**Tachometers** are sometimes used to provide an analog signal proportional to the shaft velocity. In the absence of such velocity sensors, the velocity feedback is derived by taking differences of sensed position over time. This **numerical differentiation** can introduce both noise and a time lag. Despite these potential problems, most manipulators are without direct velocity sensing.

## 8.9 FORCE SENSING

A variety of devices have been designed to measure forces of contact between a manipulator's end-effector and the environment that it touches. Most such sensors make use of sensing elements called **strain gauges**, of either the semiconductor or the metal-foil variety. These strain gauges are bonded to a metal structure and produce an output proportional to the strain in the metal. In this type of force-sensor design, the issues the designer must address include the following:

1. How many sensors are needed to resolve the desired information?
2. How are the sensors mounted relative to each other on the structure?
3. What structure allows good sensitivity while maintaining stiffness?
4. How can protection against mechanical overload be built into the device?

There are three places where such sensors are usually placed on a manipulator:

1. At the joint actuators. These sensors measure the torque or force output of the actuator/reduction itself. These are useful for some control schemes, but usually do not provide good sensing of contact between the end-effector and the environment.
2. Between the end-effector and last joint of the manipulator. These sensors are usually referred to as **wrist sensors**. They are mechanical structures instrumented with strain gauges, which can measure the forces and torques acting on the end-effector. Typically, these sensors are capable of measuring from three to six components of the force/torque vector acting on the end-effector.
3. At the “fingertips” of the end-effector. Usually, these **force-sensing fingers** have built-in strain gauges to measure from one to four components of force acting at each fingertip.

As an example, Fig. 8.19 is a drawing of the internal structure of a popular style of wrist-force sensor designed by Scheinman [22]. Bonded to the cross-bar structure of the device are eight pairs of semiconductor strain gauges. Each pair is wired in a voltage-divider arrangement. Each time the wrist is queried, eight analog voltages are digitized and read into the computer. Calibration schemes have been designed with which to arrive at a constant  $6 \times 8$  **calibration matrix** that maps these eight strain measurements into the force–torque vector,  $\mathcal{F}$ , acting on the end-effector. The sensed force–torque vector can be transformed to a reference frame of interest, as we saw in Example 5.8.

### Force-sensor design issues

Use of strain gauges to measure force relies on measuring the deflection of a stressed **flexure**. Therefore, one of the primary design trade-offs is between the stiffness and the sensitivity of the sensor. A stiffer sensor is inherently less sensitive.

The stiffness of the sensor also affects the construction of **overload protection**. Strain gauges can be damaged by impact loading and therefore must be protected against such overloads. Transducer damage can be prevented by having **limit stops**,

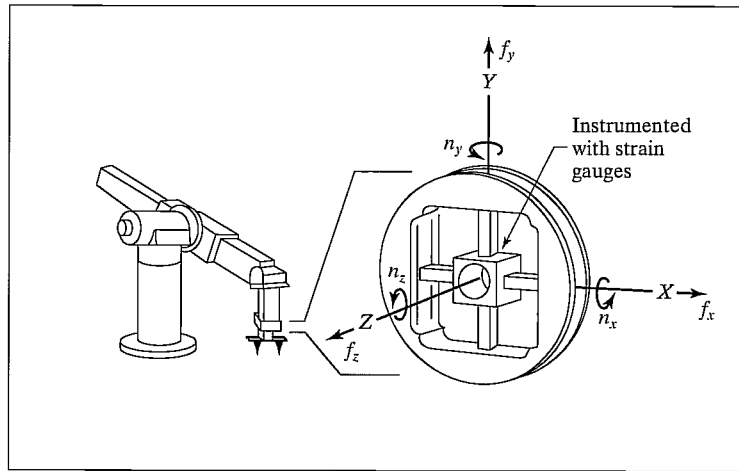


FIGURE 8.19: The internal structure of a typical force-sensing wrist.

which prevent the flexures from deflecting past a certain point. Unfortunately, a very stiff sensor might deflect only a few ten-thousandths of an inch. Manufacturing limit stops with such small clearances is very difficult. Consequently, for many types of transducers, a certain amount of flexibility *must* be built-in in order to make possible effective limit stops.

Eliminating **hysteresis** is one of the most cumbersome restrictions in the sensor design. Most metals used as flexures, if not overstrained, have very little hysteresis. However, bolted, press-fit, or welded joints near the flexure introduce hysteresis. Ideally, the flexure and the material near it are made from a single piece of metal.

It is also important to use differential measurements to increase the linearity and disturbance rejection of torque sensors. Different physical configurations of transducers can eliminate influences due to temperature effects and off-axis forces.

Foil gauges are relatively durable, but they produce a very small resistance change at full strain. Eliminating noise in the strain-gauge cabling and amplification electronics is of crucial importance for a good dynamic range.

Semiconductor strain gauges are much more susceptible to damage through overload. In their favor, they produce a resistance change about seventy times that of foil gauges for a given strain. This makes the task of signal processing much simpler for a given dynamic range.

## BIBLIOGRAPHY

- [1] W. Rowe, Editor, *Robotics Technical Directory 1986*, Instrument Society of America, Research Triangle Park, NC, 1986.
- [2] R. Vijaykumar and K. Waldron, "Geometric Optimization of Manipulator Structures for Working Volume and Dexterity," *International Journal of Robotics Research*, Vol. 5, No. 2, 1986.
- [3] K. Waldron, "Design of Arms," in *The International Encyclopedia of Robotics*, R. Dorf and S. Nof, Editors, John Wiley and Sons, New York, 1988.

- [4] T. Yoshikawa, "Manipulability of Robotic Mechanisms," *The International Journal of Robotics Research*, Vol. 4, No. 2, MIT Press, Cambridge, MA, 1985.
- [5] H. Asada, "Dynamic Analysis and Design of Robot Manipulators Using Inertia Ellipsoids," *Proceedings of the IEEE International Conference on Robotics*, Atlanta, March 1984.
- [6] J.K. Salisbury and J. Craig, "Articulated Hands: Force Control and Kinematic Issues," *The International Journal of Robotics Research*, Vol. 1, No. 1, 1982.
- [7] O. Khatib and J. Burdick, "Optimization of Dynamics in Manipulator Design: The Operational Space Formulation," *International Journal of Robotics and Automation*, Vol. 2, No. 2, IASTED, 1987.
- [8] T. Yoshikawa, "Dynamic Manipulability of Robot Manipulators," *Proceedings of the IEEE International Conference on Robotics and Automation*, St. Louis, March 1985.
- [9] J. Trevelyan, P. Kovesi, and M. Ong, "Motion Control for a Sheep Shearing Robot," *The 1st International Symposium of Robotics Research*, MIT Press, Cambridge, MA, 1984.
- [10] P. Marchal, J. Cornu, and J. Detriche, "Self Adaptive Arc Welding Operation by Means of an Automatic Joint Following System," *Proceedings of the 4th Symposium on Theory and Practice of Robots and Manipulators*, Zaburów, Poland, September 1981.
- [11] J.M. Hollerbach, "Optimum Kinematic Design for a Seven Degree of Freedom Manipulator," *Proceedings of the 2nd International Symposium of Robotics Research*, Kyoto, Japan, August 1984.
- [12] K. Waldron and J. Reidy, "A Study of Kinematically Redundant Manipulator Structure," *Proceedings of the IEEE Robotics and Automation Conference*, San Francisco, April 1986.
- [13] V. Milenkovic, "New Nonsingular Robot Wrist Design," *Proceedings of the Robots 11 / 17th ISIR Conference*, SME, 1987.
- [14] E. Rivin, *Mechanical Design of Robots*, McGraw-Hill, New York, 1988.
- [15] T. Yoshikawa, "Manipulability of Robotic Mechanisms," in *Proceedings of the 2nd International Symposium on Robotics Research*, Kyoto, Japan, 1984.
- [16] M. Leu, V. Dukowski, and K. Wang, "An Analytical and Experimental Study of the Stiffness of Robot Manipulators with Parallel Mechanisms," in *Robotics and Manufacturing Automation*, M. Donath and M. Leu, Editors, ASME, New York, 1985.
- [17] K. Hunt, *Kinematic Geometry of Mechanisms*, Cambridge University Press, Cambridge, MA, 1978.
- [18] H. Asada and K. Youcef-Toumi, *Design of Direct Drive Manipulators*, MIT Press, Cambridge, MA, 1987.
- [19] J. Shigley, *Mechanical Engineering Design*, 3rd edition, McGraw-Hill, New York, 1977.
- [20] D. Welbourne, "Fundamental Knowledge of Gear Noise—A Survey," *Proceedings of the Conference on Noise and Vibrations of Engines and Transmissions*, Institute of Mechanical Engineers, Cranfield, UK, 1979.
- [21] O. Zienkiewicz, *The Finite Element Method*, 3rd edition, McGraw-Hill, New York, 1977.

- [22] V. Scheinman, "Design of a Computer Controlled Manipulator," M.S. Thesis, Mechanical Engineering Department, Stanford University, 1969.
- [23] K. Lau, N. Dagalakis, and D. Meyers, "Testing," in *The International Encyclopedia of Robotics*, R. Dorf and S. Nof, Editors, John Wiley and Sons, New York, 1988.
- [24] M. Roshiem, "Wrists," in *The International Encyclopedia of Robotics*, R. Dorf and S. Nof, Editors, John Wiley and Sons, New York, 1988.
- [25] A. Bowling and O. Khatib, "Robot Acceleration Capability: The Actuation Efficiency Measure," *Proceedings of the IEEE International Conference on Robotics and Automation*, San Francisco, April 2000.

## EXERCISES

- 8.1 [15] A robot is to be used for positioning a laser cutting device. The laser produces a pinpoint, nondivergent beam. For general cutting tasks, how many degrees of freedom does the positioning robot need? Justify your answer.
- 8.2 [15] Sketch a possible joint configuration for the laser-positioning robot of Exercise 8.1, assuming that it will be used primarily for cutting at odd angles through 1-inch-thick, 8 × 8-foot plates.
- 8.3 [17] For a spherical robot like that of Fig. 8.6, if joints 1 and 2 have no limits and joint 3 has lower limit  $l$  and upper limit  $u$ , find the structural length index,  $Q_L$ , for the wrist point of this robot.
- 8.4 [25] A steel shaft of length 30 cm and diameter 0.2 cm drives the input gear of a reduction having  $\eta = 8$ . The output gear drives a steel shaft having length 30 cm and diameter 0.3 cm. If the gears introduce no compliance of their own, what is the overall stiffness of the transmission system?
- 8.5 [20] In Fig. 8.20, a link is driven through a shaft after a gear reduction. Model the link as rigid with mass of 10 Kg located at a point 30 cm from the shaft axis. Assume that the gears are rigid and that the reduction,  $\eta$ , is large. The shaft is steel and must be 30 cm long. If the design specifications call for the center of link mass to undergo accelerations of 2.0 g, what should the shaft diameter be to limit dynamic deflections to 0.1 radian at the joint angle?

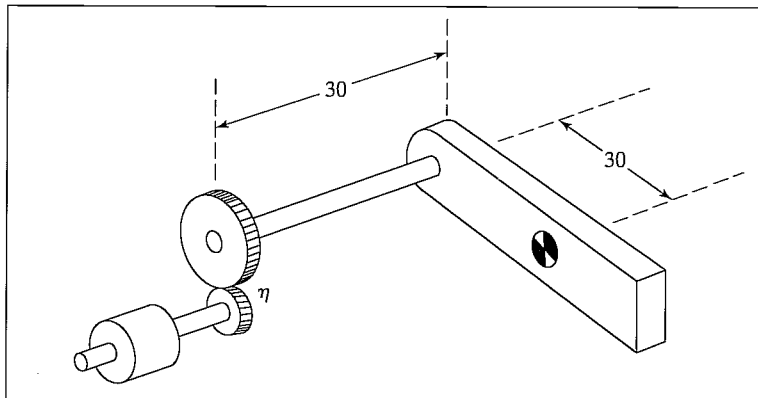


FIGURE 8.20: A link actuated through a shaft after a gear reduction.

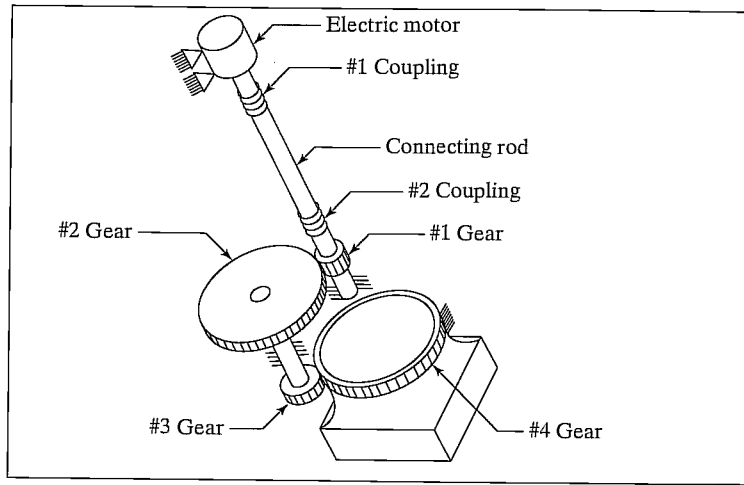


FIGURE 8.21: Simplified version of the drive train of joint 4 of the PUMA 560 manipulator (from [23]). From *International Encyclopedia of Robotics*, by R. Dorf and S. Nof, editors. From “Testing,” by K. Law, N. Dagalakis, and D. Myers.

- 8.6** [15] If the output gear exhibits a stiffness of 1000 Nt-m/radian with input gear locked and the shaft has stiffness of 300 Nt-m/radian, what is the combined stiffness of the drive system in Fig. 8.20?
- 8.7** [43] Pieper’s criteria for serial-link manipulators state that the manipulator will be solvable if three consecutive axes intersect at a single point or are parallel. This is based on the idea that inverse kinematics can be decoupled by looking at the position of the wrist point independently from the orientation of the wrist frame. Propose a similar result for the Stewart mechanism in Fig. 8.14, to allow the forward kinematic solution to be similarly decoupled.
- 8.8** [20] In the Stewart mechanism of Fig. 8.14, if the 2-DOF universal joints at the base were replaced with 3-DOF ball-and-socket joints, what would the total number of degrees of freedom of the mechanism be? Use Grübler’s formula.
- 8.9** [22] Figure 8.21 shows a simplified schematic of the drive system of joint 4 of the PUMA 560 [23]. The torsional stiffness of the couplings is 100 Nt-m/radian each, that of the shaft is 400 Nt-m/radian, and each of the reduction pairs has been measured to have output stiffness of 2000 Nt-m/radian with its input gears fixed. Both the first and second reductions have  $\eta = 6$ .<sup>2</sup> Assuming the structure and bearing are perfectly rigid, what is the stiffness of the joint (i.e., when the motor’s shaft is locked)?
- 8.10** [25] What is the error if one approximates the answer to Exercise 8.9 by considering just the stiffness of the final speed-reduction gearing?
- 8.11** [20] Figure 4.14 shows an orthogonal-axis wrist and a nonorthogonal wrist. The orthogonal-axis wrist has link twists of magnitude  $90^\circ$ ; the nonorthogonal wrist has link twists of  $\phi$  and  $180^\circ - \phi$  in magnitude. Describe the set of orientations that are *unattainable* with the nonorthogonal mechanism. Assume that all axes can turn  $360^\circ$  and that links can pass through one another if need be (i.e., workspace is not limited by self-collision).

<sup>2</sup>None of the numerical values in this exercise is meant to be realistic!

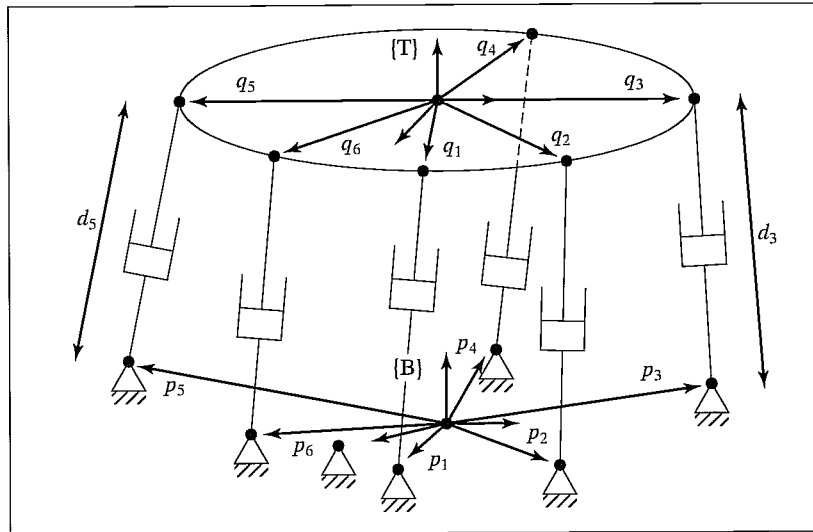


FIGURE 8.22: Stewart mechanism of Exercise 8.12.

- 8.12** [18] Write down a general inverse-kinematic solution for the Stewart mechanism shown in Fig. 8.22. Given the location of  $\{T\}$  relative to the base frame  $\{B\}$ , solve for the joint-position variables  $d_1$  through  $d_6$ . The  ${}^B p_i$  are  $3 \times 1$  vectors which locate the base connections of the linear actuators relative to frame  $\{B\}$ . The  ${}^T q_i$  are  $3 \times 1$  vectors which locate the upper connections of the linear actuators relative to the frame  $\{T\}$ .
- 8.13** [20] The planar two-link of example 5.3 has the determinant of its Jacobian given by

$$\det(J(\Theta)) = l_1 l_2 s_2. \quad (8.31)$$

If the sum of the two link lengths,  $l_1 + l_2$ , is constrained to be equal to a constant, what should the relative lengths be in order to maximize the manipulator's manipulability as defined by (8.6)?

- 8.14** [28] For a SCARA robot, given that the sum of the link lengths of link 1 and link 2 must be constant, what is the optimal choice of relative length in terms of the manipulability index given in (8.6)? Solving Exercise 8.13 first could be helpful.
- 8.15** [35] Show that the manipulability measure defined in (8.6) is also equal to the product of the eigenvalues of  $J(\Theta)$ .
- 8.16** [15] What is the torsional stiffness of a 40-cm aluminum rod with radius 0.1 cm?
- 8.17** [5] What is the effective "gear" reduction,  $\eta$ , of a belt system having an input pulley of radius 2.0 cm and an output pulley of radius 12.0 cm?
- 8.18** [10] How many degrees of freedom are required in a manipulator used to place cylindrical-shaped parts on a flat plane? The cylindrical parts are perfectly symmetrical about their main axes.
- 8.19** [25] Figure 8.23 shows a three-fingered hand grasping an object. Each finger has three single-degree-of-freedom joints. The contact points between fingertips and the object are modeled as "point contact"—that is, the position is fixed, but the relative orientation is free in all three degrees of freedom. Hence, these point contacts can be replaced by 3-DOF ball-and-socket joints for the purposes of

analysis. Apply Grübler's formula to compute how many degrees of freedom the overall system possesses.

- 8.20** [23] Figure 8.24 shows an object connected to the ground with three rods. Each rod is connected to the object with a 2-DOF universal joint and to the ground with a 3-DOF ball-and-socket joint. How many degrees of freedom does the system possess?

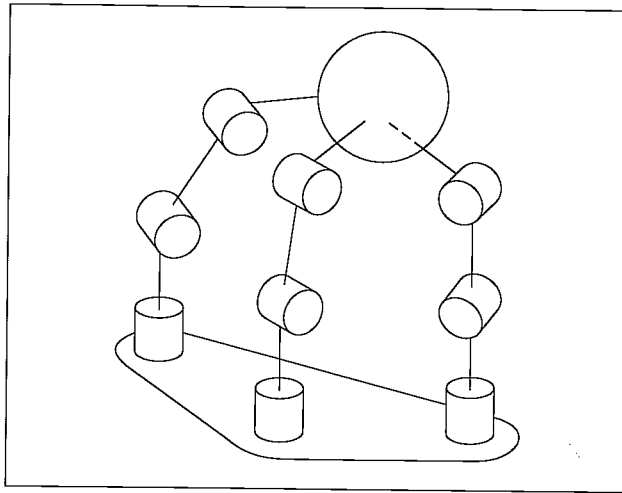


FIGURE 8.23: A three-fingered hand in which each finger has three degrees of freedom grasps an object with “point contact.”

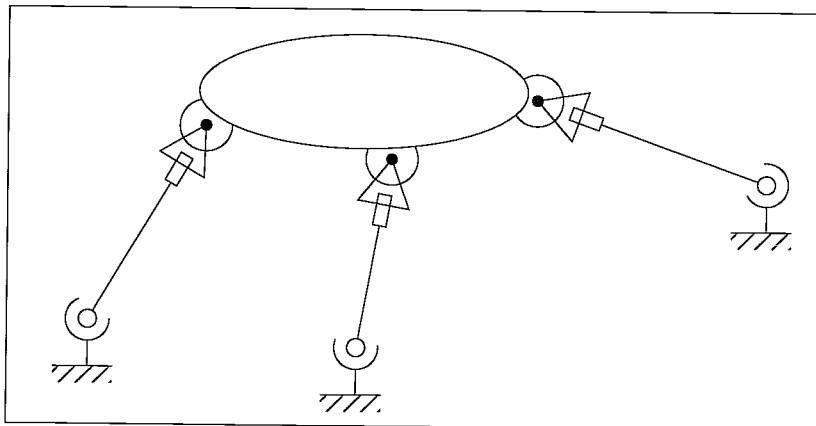


FIGURE 8.24: Closed loop mechanism of Exercise 8.20.

- 8.21** [18] Verify that, if two transmission systems are connected serially, then the equivalent stiffness of the overall system is given by (8.14). It is perhaps simplest to think of the serial connection of two linear springs having stiffness coefficients

$k_1$  and  $k_2$  and of the resulting equations:

$$\begin{aligned} f &= k_1 \delta x_1, \\ f &= k_2 \delta x_2, \\ f &= k_{\text{sum}}(\delta x_1 + \delta x_2). \end{aligned} \tag{8.32}$$

- 8.22** [20] Derive a formula for the stiffness of a belt-drive system in terms of the pulley radii ( $r_1$  and  $r_2$ ) and the center-to-center distance between the pulleys,  $d_c$ . Start from (8.22).

### PROGRAMMING EXERCISE (PART 8)

1. Write a program to compute the determinant of a  $3 \times 3$  matrix.
2. Write a program to move the simulated three-link robot in 20 steps in a straight line and constant orientation from

$${}^0_3T = \begin{bmatrix} 0.25 \\ 0.0 \\ 0.0 \end{bmatrix}$$

to

$${}^0_3T = \begin{bmatrix} 0.95 \\ 0.0 \\ 0.0 \end{bmatrix}$$

in increments of 0.05 meter. At each location, compute the manipulability measure for the robot at that configuration (i.e., the determinant of the Jacobian). List, or, better yet, make a plot of the values as a function of the position along the  $\hat{X}_0$  axis. Generate the preceding data for two cases:

- (a)  $l_1 = l_2 = 0.5$  meter, and
- (b)  $l_1 = 0.625$  meter,  $l_2 = 0.375$  meter.

Which manipulator design do you think is better? Explain your answer.

### MATLAB EXERCISE 8

Section 8.5 introduced the concept of kinematically redundant robots. This exercise deals with the resolved-rate control simulation for a kinematically redundant robot. We will focus on the planar 4-DOF 4R robot with one degree of kinematic redundancy (four joints to provide three Cartesian motions: two translations and one rotation). This robot is obtained by adding a fourth R-joint and a fourth moving link  $L_4$  to the planar 3-DOF, 3R robot (of Figures 3.6 and 3.7; the DH parameters can be extended by adding one row to Figure 3.8).

For the planar 4R robot, derive analytical expressions for the  $3 \times 4$  Jacobian matrix; then, perform resolved-rate control simulation in MATLAB (as in MATLAB Exercise 5). The form of the velocity equation is again  ${}^k\dot{X} = {}^k J \dot{\Theta}$ ; however, this equation cannot be inverted by means of the normal matrix inverse, because the Jacobian matrix is nonsquare (three equations, four unknowns, infinite solutions to  $\dot{\Theta}$ ). Therefore, let us use the Moore–Penrose pseudoinverse  $J^*$  of the Jacobian matrix:  $J^* = J^T (J J^T)^{-1}$ . For the resulting commanded relative joint rates for the resolved-rate algorithm,  $\dot{\Theta} = {}^k J^* \dot{X}$ ,

choose the minimum-norm solution from the infinite possibilities (i.e., this specific  $\dot{\Theta}$  is as small as possible to satisfy the commanded Cartesian velocities  ${}^k\dot{X}$ ).

This solution represents the particular solution only—that is, there exists a homogeneous solution to optimize performance (such as avoiding manipulator singularities or avoiding joint limits) in addition to satisfying the commanded Cartesian motion. Performance optimization is beyond the scope of this exercise.

Given:  $L_1 = 1.0\text{ m}$ ,  $L_2 = 1.0\text{ m}$ ,  $L_3 = 0.2\text{ m}$ ,  $L_4 = 0.2\text{ m}$ .

The initial angles are:

$$\Theta = \begin{Bmatrix} \theta_1 \\ \theta_2 \\ \theta_3 \\ \theta_4 \end{Bmatrix} = \begin{Bmatrix} -30^\circ \\ 70^\circ \\ 30^\circ \\ 40^\circ \end{Bmatrix}.$$

The (constant) commanded Cartesian velocity is

$${}^0\dot{X} = {}^0 \begin{Bmatrix} \dot{x} \\ \dot{y} \\ \omega_z \end{Bmatrix} = \begin{Bmatrix} -0.2 \\ -0.2 \\ 0.2 \end{Bmatrix} \text{ (m/s, rad/s)}.$$

Simulate resolved-rate motion, for the particular solution only, for 3 sec, with a control time step of 0.1 sec. Also, in the same loop, animate the robot to the screen during each time step, so that you can watch the simulated motion to verify that it is correct.

**a)** Present four plots (each set on a separate graph, please):

1. the four joint angles (degrees)  $\Theta = \{\theta_1 \ \theta_2 \ \theta_3 \ \theta_4\}^T$  vs. time;
2. the four joint rates (rad/s)  $\dot{\Theta} = \{\dot{\theta}_1 \ \dot{\theta}_2 \ \dot{\theta}_3 \ \dot{\theta}_4\}^T$  vs. time;
3. the joint-rate Euclidean norm  $\|\dot{\Theta}\|$  (vector magnitude) vs. time;
4. the three Cartesian components of  ${}^0_H T, X = \{x \ y \ \phi\}^T$  (rad is fine for  $\phi$  so that it will fit) vs. time.

Carefully label (by hand is fine!) each component on each plot. Also, label the axis names and units.

**b)** Check your Jacobian matrix results for the initial and final joint-angle sets by means of the Corke MATLAB Robotics Toolbox. Try function `jacob0()`. **Caution:** The toolbox Jacobian functions are for motion of {4} with respect to {0}, not for {H} with respect to {0} as in the problem assignment. The preceding function gives the Jacobian result in {0} coordinates; `jacobn()` would give results in {4} coordinates.